Sun photometer for scientific monitoring (instrumentation, techniques, algorithms)

D.M. Kabanov, S.M. Sakerin, and S.A. Turchinovich

Institute of Atmospheric Optics,
Siberian Branch of the Russian Academy of Sciences, Tomsk

Received November 5, 2001

The paper presents a description of a multi-wave sun photometer intended for all-the year-round automated measurements of the atmospheric transparency in the wavelength range 0.37–4 μm. The instrumentation complex is capable of determining the aerosol optical thickness (AOT), moisture content, direct and total solar radiation. The methods of automation of the experiment, calibration of the photometer, and calculation of AOT of the atmosphere are under consideration.

Introduction

The method of sun photometry of the atmosphere has a rich history and is well known in atmospheric optical investigations. It allows one: 1) to measure direct radiation in different wavelength ranges, 2) to determine the aerosol optical thickness (AOT) of the atmosphere in the transparency windows, 3) to determine the total content of gases in their absorption bands (differential technique), and 4) to measure the angular and polarization characteristics of the scattered light. In addition, it makes possible to retrieve the aerosol microphysical characteristics by solving the inverse problem.

The important stage of development of the method was the organization of monitoring of the atmospheric AOT and total ozone content at the network of stations working under the aegis of WMO and equipped with the standard sun photometers (MS–115 (Japan), SPUV–6 (USA), PFR (Switzerland), etc. are among them). Uniform methods of observation and data processing made it possible to obtain numerous data on variations of the atmospheric transparency in the wavelength range 0.38 to 0.87 μm in different regions of the planet. (unfortunately, in the last few years the network observations in Russia were practically stopped). In parallel with the network photometers, some devices were developed in scientific institutions for solving a wider range of problems through extension of the spectral region, measurements of angular characteristics, etc.

The method of sun photometry has such advantages as simplicity and information capacity, but its realization is possible only during the periods when the Sun is not hidden by clouds. This drawback restricts the applicability of the method and the possibility of automation of the experiment, especially at all-the-year-round monitoring. It is relatively easy to realize technically the main functions of the photometer (guidance to the Sun, replacing of the light filters (or scanning the spectrum), recording of the signals), but it is difficult to make a decision about beginning (stopping) measurements without attention. The use of computer technologies in experimental investigations presents a possibility of overcoming this difficulty.

In this paper, the SP–4m multiwave sun photometer destined for automated all-the-year-round measurements of atmospheric transparency in a wide wavelength range is described. Besides, we think that it is expedient to generalize the methods for calibration and measurements, some of which were not described in our previous papers.[1,2]

1. Design of the sun photometer

When creating the SP–4m sun photometer (Figs. 1 and 2) we took into account our experience of operation and some technical solutions of its earlier modifications.[2,3] The sun photometer consists of two separate blocks linked by a cable. The optical-electronic block is mounted outdoors on a two-coordinate (azimuth-zenith) rotating table. The power-supply block, remote control panel, computer, analog-to-digital and digital-to-analog converters (ADC/DAC) are situated indoors. The photometer includes three measurement channels adjusted in one direction, – the shortwave (SW) channel with siliceous photodiode, the longwave (LW) channel with pyroelectric detector, and the M–3 built-in actinometer. The measurement complex also includes the PP–1 pyranometer with a device for remote opening the protective cover[4] and the sensor of illumination (standard photodiode with scattering nozzle), which are mounted near the photometer. The standard M–3 and PP–1 actinometric devices measure the total and direct solar radiation in the wavelength range ~ 0.3 to 3 μm.

Optical schemes of the measurement channels are lensless, the angles of view are formed by the field diaphragms mounted in the blends in front of the inlet windows. Spectral selection of solar radiation is performed by means of interference filters mounted in the continuously rotating drum. When the due filters

0235-6880/01/12 1067-08 $02.00

cross the optical axis, the electronic circuit with optronic pairs produces the service signals which make it possible to sort the signals of transparency according to the wavelengths. A plug is installed instead of one of the filters for continuous monitoring of noise and possible adjacent lights. The incoming radiation in LW channel is firstly modulated by an electromechanic modulator with the stabilization scheme, and then is amplified by a selective amplifier and detected. The measurement and service signals are transmitted through the screened cable to ADC and recorded by the computer.

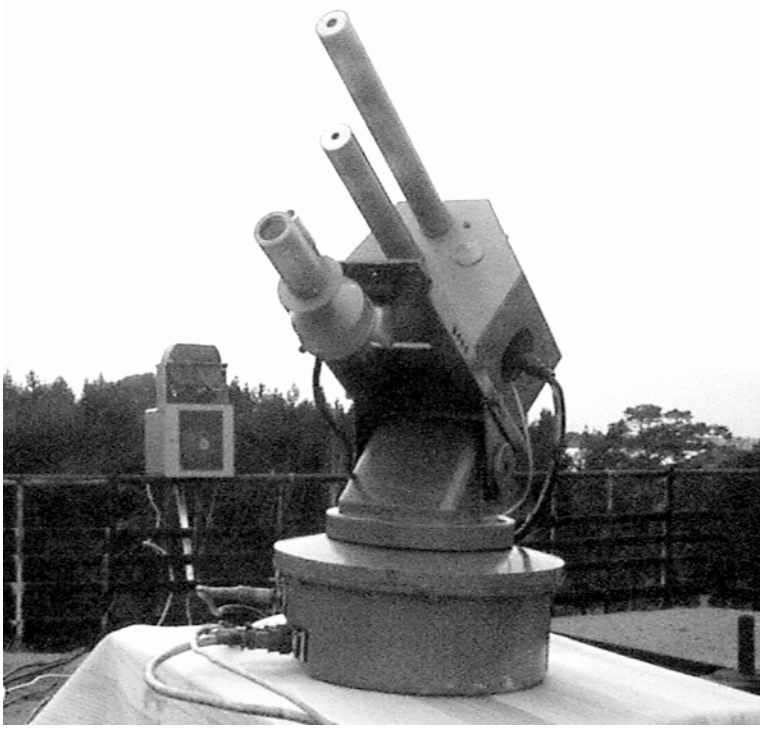

Fig. 1. External view of the SP–4m sun photometer.

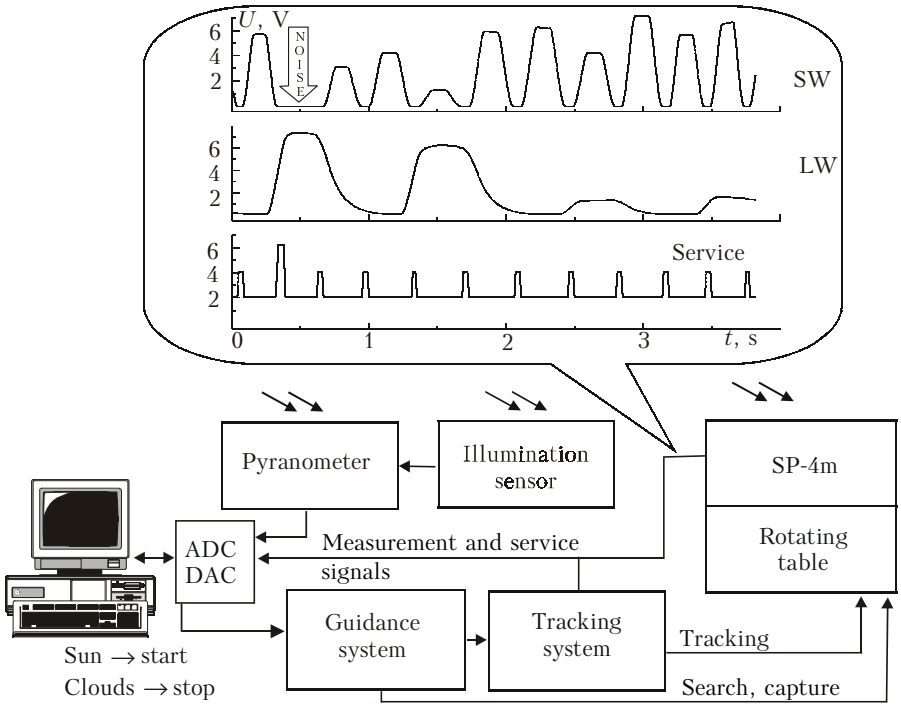

Fig. 2. The experimental complex and conventional diagram of the SP–4m sun photometer operation (the diagram of service and measurements signals is in the frame).

To decrease the effect of external factors (humidity, temperature, stray electromagnetic currents) the optical-electronic block is placed into the double protective housing. The internal humidity-protected one has the scheme of thermostating and heating the inlet windows. The external housing serves to protect against precipitation and additional heating of the photometer in winter. Principal specifications of the designed photometer are presented in Table 1.

Table 1. Specifications of the SP–4m sun photometer

Characteristics	SW channel	LW channel
Central angle of the field of view, deg	1.38	1.48
Number of wavelengths	10	4
Maxima of the light filter transmission bands, μm	0.371; 0.408; 0.438; 0.475; 0.500; 0.547; 0.675; 0.871; 0.938; 1.052	1.246; 1.557; 2.20; 3.97
Halfwidth of the filter transmission, nm	5–12	15–40
Type of photoreceiver	FD–24k	MG-32
Error in photometering, %	0.3	0.7
Error in sun tracking, deg	0.2	
"Spectrum" measurement duration (1 revolution of the drum), sec	5	
Range of the guidance angles (zenith×azimuth), deg	90×300	
Thermostat temperature, °C	32 ± 0.3	
Range of surrounding temperature, °C	from –50 to 35	
Total mass of the photometer (estimate), kg	30	
Measurable characteristics (range/error):		
aerosol optical thickness;	0 – 1/0.01	
atmospheric moisture content, g/cm^2;	0 – 6/0.07	
direct, total, and scattered radiation, W/m^2	0 – 1500/6%	

2. Technique for calibration and determination of AOT

Our technique for determination of AOT was considered earlier,[1] so we restrict ourselves to its concise characteristics, and will pay our principal attention to the calibration.

As is known, the method of sun photometry is based on the Bouguer–Lambert law, which relates the measured direct solar radiation to the atmospheric transparency:

$$U_\lambda = \rho U_{0\lambda} T_\lambda^\Sigma = \rho U_{0\lambda} T_\lambda^W T_\lambda^X T_\lambda^C \exp[-M(\tau_\lambda^R + \tau_\lambda^A)] , \quad (1)$$

where $M(Z)$ is the atmospheric air mass at the zenith angle Z of the Sun, ρ is the correction for the annual change of the distance to the Sun, U_λ are the measured signals of direct radiation at different wavelengths λ, $U_{0\lambda}$ are the extra-atmospheric values of the signals (calibration constants), T_λ^Σ, T_λ^W, T_λ^X, T_λ^C are the atmospheric transmission functions (total, water vapor, ozone, and "constant" gases, respectively); τ_λ^R is the optical thickness of the molecular (Rayleigh) scattering, and τ_λ^A is the aerosol optical thickness.

The peculiarity of the technique[1] is that exclusion of the molecular absorption and scattering is performed at the initial stage by dividing the measured signals into the transmission functions $T_{\Delta\lambda}^j$ for each jth spectral channel. The transmission functions $T_{\Delta\lambda}^j$ are calculated by the LOWTRAN–7 model[5] taking into account the real variability of the gaseous components (H_2O, O_3) and the spectral instrumental function of the photometer A_λ (spectra of the Sun, transmission of filters, and input windows):

$$T_{\Delta\lambda}^j = \int A_\lambda T_\lambda^W T_\lambda^X T_\lambda^C T_\lambda^R d\lambda \Big/ \int A_\lambda d\lambda . \quad (2)$$

Table 2 gives the general idea of the magnitudes of molecular absorption and scattering in different (jth) spectral channels. The optical thickness $\tau_j^G = \ln T_{\Delta\lambda}^j$ for mid-latitude summer at $M = 1$ is also presented here.

After going to the aerosol signals $Y_\lambda^j = U_\lambda / T_{\Delta\lambda}^j$ (see below), the calibration is performed and the sought values of AOT of the atmosphere are determined:

$$\tau_\lambda^A = M^{-1} \ln(U_{0\lambda} / Y_\lambda^j) . \quad (3)$$

Note that the transmission functions of different components of the atmosphere together with their optical masses M_i are calculated separately. Therefore, the considered technique allows relatively simple extension of the measurement range up to great zenith angles taking into account the individual dependence $M_i(Z)$.[6]

The error in determining τ_λ^A significantly depends on the carefulness of the calibration. The essence of the calibration lies in extrapolation of the dependences $\ln U_\lambda = f(M)$ to the mass $M = 0$ (the Bouguer method).[7] The majority of researchers dealing with the atmospheric transparency[8–10,etc.] were engaged in improvement and development of new techniques for determining $U_{0\lambda}$. Recall that selection of measurement days, meeting the conditions of the stable atmosphere, high transparency, and wide range of air masses, is necessary for performing the calibration. There appear some difficulties in "manual" selection of data and

Table 2. Optical thicknesses τ_j^G and τ_λ^R for the SP–4m sun photometer

λ, μm	0.371	0.408	0.438	0.475	0.500	0.547	0.675	0.871	1.052	1.246	1.557	2.20	3.97
τ_j^G	0	0	0.002	0.005	0.010	0.026	0.032	0.082	0.044	0.053	0.060	0.188	0.217
τ_λ^R	0.499	0.328	0.244	0.175	0.143	0.102	0.042	0.014	0.008	0.003	0.001	0	0

construction of the calibration plots[7] (see the example in Fig. 3) at routine multiwave measurements. Therefore, the iteration technique for calculation of $U_{0\lambda}$ was developed.[11]

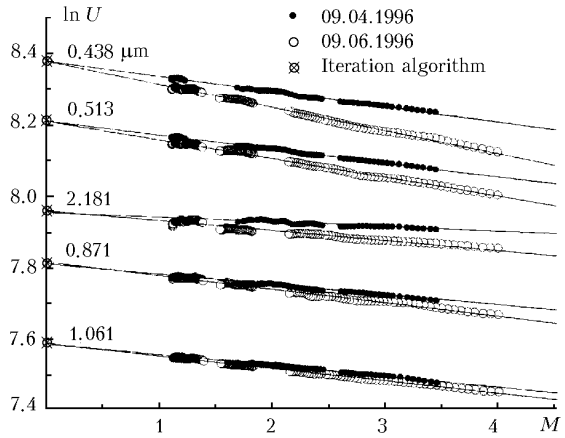

Fig. 3. Illustration of the calibration straight lines constructed by the Bouguer method (points on the ordinate axis show the values $U_{0\lambda}$ calculated by the iteration method).

The algorithm is based on the fact that the minimum dependence of τ_λ^A on time of day and the air mass should take place under conditions of high transparency of the atmosphere. Variations of τ_λ^A at its minimum values become comparable with the measuring errors. In this case the sought U_0^* and the true U_0 values of the calibration constants can be related by the relationship $U_0^* = U_0(1+k)$, and one can use the following regression equation when selecting U_0^*:

$$\tau^* = \nu + (\varepsilon \pm \delta_\varepsilon)\, M^{-1}, \qquad (4)$$

where ε and δ_ε correspond to systematic and random errors in selecting U_0.

The quality of selection of U_0^* was determined in the dialog regime using the shape of the displayed dependence $\varepsilon(\tau_i^*)$, where τ_i^* is the variable upper boundary of the subset of optical thicknesses ($\tau^* < \tau_i^*$), by which ε was calculated. The criterion was the convergence to zero of the values $\varepsilon(\tau_i^*)$ when τ_i^* decreased. To exclude the subjectivity of the dialog technique, the algorithm was developed on the basis of the formal criterion for selection of U_0^*. The following quantities were used in calculations:

$$\Theta = \sum_{j=1}^{10} |\,\varepsilon(\tau_j^*)\,| \quad , \quad \delta_\Theta = \sqrt{\sum_{j=1}^{10} \delta_\varepsilon^2(\tau_j^*)}\,, \qquad (5)$$

where ε was determined in the subset $\tau_{\min}^* \le \tau^* \le \tau_j^*$, $\tau_j^* = \tau_{\min}^* + 0.005j$ under condition that the number of experimental points falling into the subset is greater than five.

The character of dependences $\Theta(U_0^*)$ and $\delta_\Theta(U_0^*)$ is shown in Fig. 4. The decrease of the calculated values $\Theta(U_0^*)$ and $\delta_\Theta(U_0^*)$ corresponds to approaching U_0^* to the true value U_0. The minima of Θ and δ_Θ correspond to the most exact selection of U_0^*. The accuracy of the developed algorithm was tested using the data array obtained earlier during the sea cruise in 1994. In this case we had a possibility to compare the calibrations calculated both by the dialog variant[11] and by the traditional technique[7] applied to the results of test measurements in mountain conditions (at the Tenerife astrophysical observatory at the height of 2.38 km). As is known, observations in mountains provide for the most reliable calibration. Comparison of the values $U_{0\lambda}$ obtained by different techniques (see Fig. 3 and Table 3) shows that the difference is not greater than ± 0.3%.

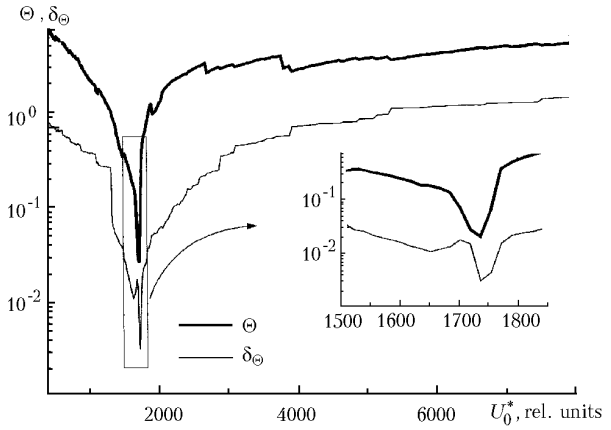

Fig. 4. Example of the dependences $\Theta(U_0^*)$ and $\delta_\Theta(U_0^*)$ obtained at the iteration calibration.

The results of one more test of the algorithm (in 1996) are presented in Table 4 in the form of relative values of the difference between the calibration signals $\Delta_i = (U_{00} - U_{0i})/U_{00}$. The indices sign the following variants of calculating Δ_i: 0 is the iteration algorithm applied to all array of data, 1 and 2 indicate forenoon and afternoon measurements; 3 and 4 denote the first and the second halves of the expedition period, and 5 is the calibration by the Bouguer method. It is seen in Table 4 that the mean deviation from the main variant (U_{00}) is ± 0.5% in the whole spectral range. Besides, from comparison of variants 3 and 4 one can draw the conclusion about sufficiently stable sensitivity of the photometer during several months of observations.

Table 3. Comparison of the calibration constants calculated by different methods

λ, μm	0.369	0.408	0.423	0.438	0.484	0.514	0.553	0.637	0.673	0.871	1.061
Bouguer method	1659	2232	2460	2294	2468	2182	1734	942	1733	1410	799
Dialog algorithm (4)	1650	2229	2450	2285	2482	2190	1730	–	–	–	–
Iteration algorithm (5)	1659	2223	2456	2286	2480	2186	1733	942	1731	1405	797
Difference in $U_{0\lambda}$, ± %	0.27	0.20	0.20	0.20	0.28	0.18	0.12	0	0.06	0.17	0.25

Table 4. Difference in the calibration signals Δ_i, %, calculated for different variants

Variant	0.369	0.408	0.423	0.438	0.484	0.514	0.553	0.637	0.673	0.871	1.061	2.18	4.0
1	−0.48	0.29	0.19	0	0	−0.19	−0.91	0	−0.19	−0.57	0.38	1.19	0
2	0.72	0.10	−0.29	−0.29	0.48	0.38	0.71	0	0.10	0.19	−0.10	−0.67	−0.96
3	0	0.67	−0.09	0.19	0.10	−1.16	0.58	−0.96	−0.96	−0.67	−0.48	0.19	0.29
4	−0.78	0.30	−0.25	0.42	−0.93	0.04	−0.30	−0.06	0.04	−0.35	−0.86	−0.34	0.01
5	−0.16	0.48	0.07	−0.01	0.06	−0.41	0.87	−0.39	−0.42	−0.78	0.16	−0.65	−0.34

Thus, with the iteration algorithm (5) the calibration procedure was significantly simplified. The condition for its realization is an accumulation of quite long series of observations with situations of high atmospheric transparency. So the main requirement to the experiment is the long-term stable operation of the sun photometer under complicated conditions of exposure to the environment.

3. System of orientation of the photometer and automation of measurements

The procedure of the experiment is in orientation of the photometer to the Sun free of clouds during its movement in the sky and measurement of the direct radiation at different wavelengths. Determination of the situations, where the Sun is not covered with clouds, and spatial orientation of the photometer are the most complicated moments for automation of measurements.

Two methods for guidance of the devices to the Sun are used in the practice of automated measurements, astronomical and optical-radar. In the first case, the orientation is performed in the direction of the calculated trajectory of the Sun movement (see, for example, Refs. 12 and 13). The second method is experimental, and guidance of the photometer is performed to the really observed Sun by means of special optical-electronic devices. Without concentrating on the analysis of the two approaches, we note that the radar method is preferable under field and mobile conditions.

The designed system of guidance and tracking the Sun is the result of development of previous devices.[2,3] It consists of four photodiodes of the scheme of rough guidance and the PD−142 four-section photodiode of the scheme of fine guidance located in a common body. Another photodiode, central, switches control from one scheme to another. The four-section photodiode is fitted in the lens focus, and the photodiodes of rough guidance are turned relative to each other to enlarge the total field of view. Optical axes of the two systems are aligned so that after operation of the rough guidance scheme the Sun comes into the view of the lens system of fine tracking. The electric drives of the turning table are controlled by means of electronic circuits of difference signals coming from the sensors of rough or fine guidance. Besides, the scheme provides for manual guidance of the photometer from the control panel. The Sun position relative to the vision direction is controlled by four photodiodes: up, down, left, and right.

A computerized pyranometer with special algorithm for processing the results of continuous measurements of total radiation is used to solve the second problem, i.e., determination of the fact of the "cloudless" Sun. The possibilities to increase the information capacity of pyranometric measurements were discussed earlier.[14] One of such possibilities is used in the considered device.

When analyzing the data on diurnal distributions of total radiation accumulated for different seasons and atmospheric conditions, it was revealed that the total field of the recorded values could be divided distinctly into two zones (Fig. 5). As the parallel instrumental-visual observations have shown, the range of higher radiation values I corresponds to the Sun free of clouds at different atmospheric transparencies, and the range of the lower values II characterizes cloudy situations. Hence, the demarcation line between two zones can be used as a threshold value $Q_n(h)$ for decision about the presence of clouds near the Sun. Taking into account the aforementioned idea, we have developed a simple algorithm which lies in continuous comparison of the measured radiation $Q_i(h)$ with the threshold $Q_n(h)$ for the calculated Sun elevation h. The efficiency of the chosen technique was tested and confirmed during a long-term experimental operation of the complex.

The general algorithm of automated operation of the photometer is explained by Fig. 2:

– at the sunrise the sensor of illumination opens the protection cover of the pyranometer and starts the program for measuring the total radiation;

– at the "cloudless" Sun the computer makes the corresponding decision, and the system of tracking the Sun (rough guidance) is switched on by the signal of DAC;

– when the Sun comes to the field of view of the central photodiode, the control for the turning table is switched to the fine tracking scheme, the sun photometer is switched on, and the program of measuring the spectral atmospheric transparency (in addition to the total radiation) starts;

– when clouds appear, the mode of measuring transparency is switched off by the service signal of DAC, and the photometer on the turning table is switched to the waiting position (down–southward). This is necessary to facilitate the subsequent process of looking for the Sun and protecting the input optics of precipitation;

– at the sunset, the sensor of illumination switches off the measurement program and closes the protection cover of the pyranometer.

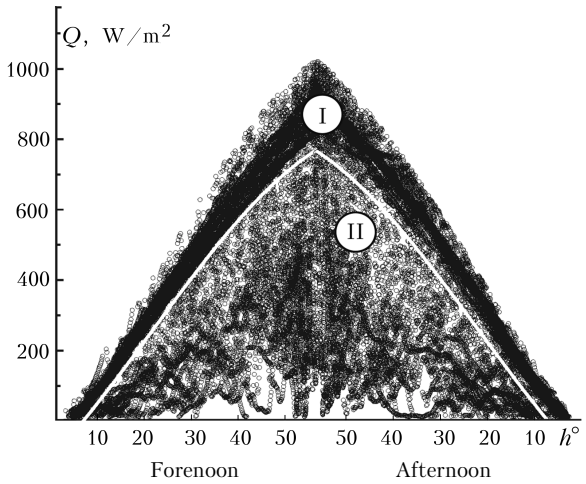

Fig. 5. Total field of the diurnal distributions of solar radiation.

The procedure of measuring the signals U_λ by the photometer of this type has a peculiarity, as it is performed at continuous rotation of the drum with interference filters. During the operation, the light flux modulation occurs simultaneously with the wavelength change (see framing in Fig. 2). The amplitude maxima in the pulse sequence correspond to the sought signals in different wavelength ranges, and the intermediate values correspond to the transition process of changing the filters. Besides, the short-time attenuation of a signal is possible during actual measurements because of occurring clouds in the field of view and inaccurate operation of the tracking system. As the result, the maxima of the recorded pulse amplitudes not always can reach their true values. The maximum value of a signal appears only in the moments when the centers of light filters are in line with the optical axis of the photoreceiver, the latter is oriented exactly to the Sun, and clouds in the field of view are absent.

The traditional averaging of signals in the considered recording scheme would not do. Therefore, the following procedure of processing the initial signals is accepted to be optimal:

1) when crossing the optical axis by the next light filter due, the ADC is interrogated and the maximum U'_λ is chosen;

2) the obtained values of U'_λ are accumulated for each wavelength during 10 turns of the filter drum (for less than 1 minute), and then the maximum signal among them U''_λ is selected;

3) after the signals U''_λ are recorded, the readings are referenced to the current time. The aforementioned procedures are computerized (see below).

The results of the data processing including the choice of maximum readings can be untrue at great noise of the photometer, but, as a rule, the signal-to-noise ratio is not less than 100. The operating experience of photometers of the SP type[2,3] confirms the efficiency of the described algorithm even under more complicated conditions, i.e., measuring solar radiation through small, quickly changing breaks in clouds.

4. Software

Automation of measurements, data preprocessing, and control for the photometer operation are provided by a software package including the following programs: measurement, editing, and testing. Composition of the majority of procedures was considered above.

The measurement program (Fig. 6) performs processing the data coming from SW, LW, and service channels of the photometer, pyranometer, and actinometer, as well as forming the data arrays and storing them on a hard disk. The program includes three modes of operation and executes the following procedures:

1. Wait for the sunrise and transition to the next mode at switching on the pyranometer.

2. Measurement of the total radiation (minute-average), and, in the case of exceeding the threshold ($Q_i > Q_n$), initiation of start of the tracking system of the photometer, and the transition to the mode 3 after capture of the Sun.

3. The mode of joint recording of the data of the photometer and the pyranometer, which includes:

– spectral selection of the transparency signals using service signals of various levels coming from the filter drum rotation system;

– automatic filtration of the readings distorted by errors in operation of the photometer (tracking system, filter drum) and short-time overlaps of the Sun by clouds;

– reference of the current reading to time, calculation of the Sun elevation angle, and the optical mass of the atmosphere;

– display of the current (daily) data in digital and plot form – Fig. 7 (at the known calibration constants, the calculated values of AOT and moisture content are displayed instead of the signals of transparency);

– current control for operation of individual elements of the photometer and exclusion of false readings caused by instrumentation failures.

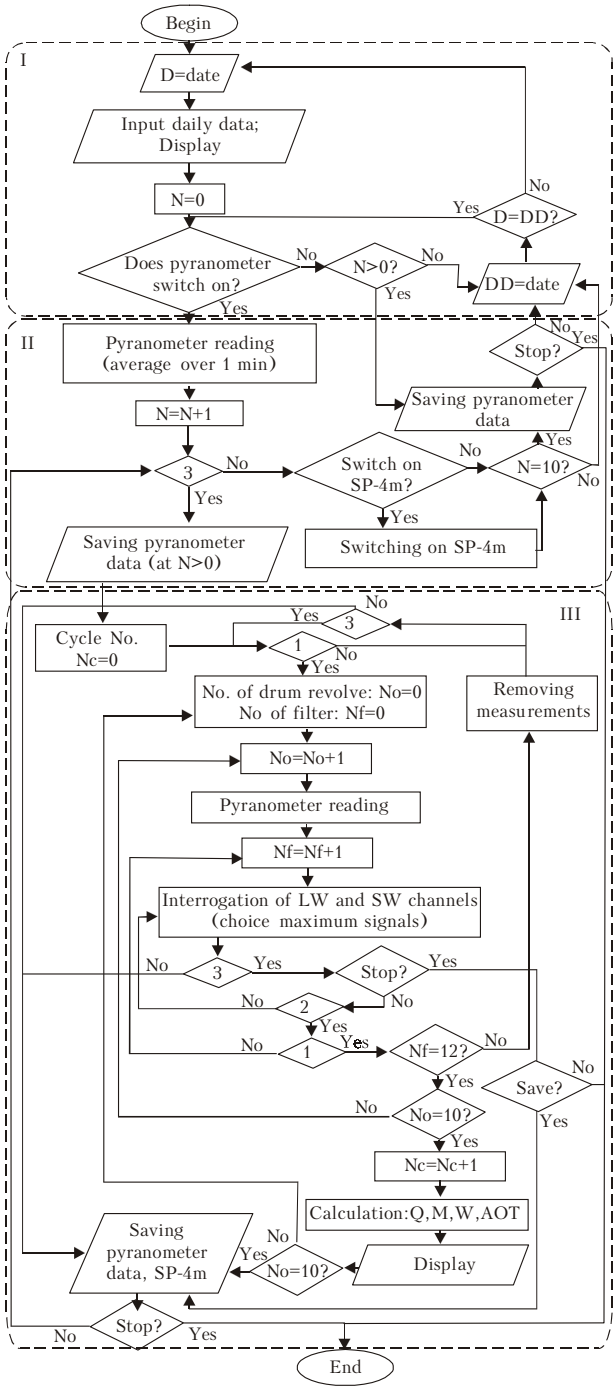

Fig. 6. Block-diagram of the measurement program: I, II are testing of the service signals "start of the turn" and "filter," III is testing of switch on the photometer.

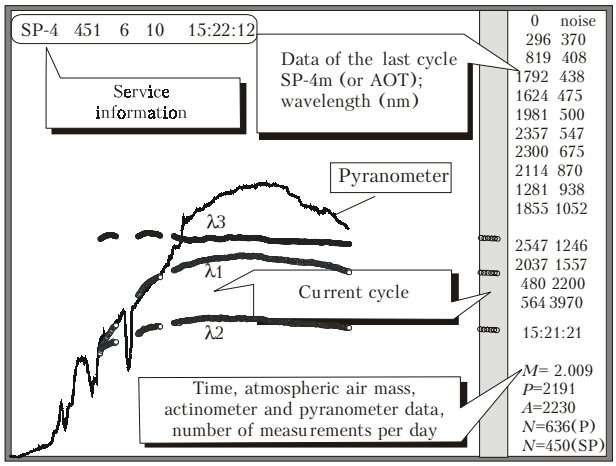

Fig. 7. A view of the data displayed during measurements.

Two files are formed during operation of the program. They include the data of the pyranometer and photometer, which are added on every 10 minutes.

The program termination is performed through the operator command with or without storing the last measurements.

The editing program is initiated every day after termination of measurements. It excludes the false readings not filtered during measurements. The rejecting is performed by the operator based on the plotted and digital data on transparency signals accumulated for the whole day or some time intervals. Two types of removing data are provided: without storage and with recording to an individual file for subsequent analysis, for example, spectral transparency of cirrus clouds.

The testing program displays all service and measurement signals in plotted and digital form without preprocessing. This is used for adjustment of some blocks and for laboratory tests.

Conclusion

The long-term operation of the SP–4m sun photometer under different conditions (including winter and precipitation) has confirmed its suitability at regular all-the-year-round measurements of the incoming radiation and atmospheric transparency. Development of the iteration algorithm for calibration of the photometer allows one to avoid high-cost observations in mountain conditions and essentially simplify (together with a number of other programs) the routine calculations in the processing of large arrays of multiwave measurements of the atmospheric transparency. In addition, the selected algorithm of automation made unneeded the continuous observations of the sky and waiting for situations of the "cloudless" Sun.

Thus, one can conclude that application of the modern computer technologies in the experiment makes it possible to organize a low-cost (from the standpoint

of costs of the staff of operators) scientific monitoring of characteristics of the atmospheric transparency.

Acknowledgments

This work was supported in part by the Russian Foundation for Basic Research (Project No. 01–05–64644) and the Inter-disciplinary integration project of SB RAS No. 56.

References

1. D.M. Kabanov and S.M. Sakerin, Atmos. Oceanic Opt. **10**, No. 8, 540–545 (1997).
2. D.M. Kabanov, S.M. Sakerin, and S.A. Turchinovich, in: *Regional Monitoring of Siberia* (Spektr, Tomsk, 1997), Part 2, pp. 131–145.
3. D.M. Kabanov, S.M. Sakerin, A.M. Sutormin, and S.A. Turchinovich, Atmos. Oceanic Opt. **6**, No. 4, 270–273 (1993).
4. S.M. Sakerin, D.M. Kabanov, and S.A. Turchinovich, Atmos. Oceanic Opt. **9**, No. 12, 1046–1052 (1996).
5. F.X. Kneizys, E.P. Shettle, L.W. Abreu, J.H. Chetwynd, J.P. Anderson, W.O. Gallery, J.E. A. Selby, and S.A. Clough, *Users Guide to LOWTRAN-7*, AFGL–TR–0177 (1988), 137 pp.
6. S.M. Sakerin and D.M. Kabanov, in: *Abstracts of Reports at IV Symposium on Atmospheric and Ocean Optics*, Tomsk (1997), pp. 155–156.
7. G.P. Gushchin, Methods, *Instruments and Results of Measurement of the Spectral Transparency of the Atmosphere* (Gidrometeoizdat, Leningrad, 1988), 200 pp.
8. B.W. Forgan, Appl. Opt. **33**, No. 12, 4841–4850 (1994).
9. V. Soufflet, C. Devaux, and D. Tanre, Appl. Opt. **31**, No. 12, 2154–2162 (1992)
10. B.M. Herman, M.A. Box, J.A. Reagan, and C.M. Evans, Appl. Opt. **20**, No. 17, 2925–2928 (1981).
11. A.M. Ignatov, I.L. Dergileva, S.M. Sakerin, and D.M. Kabanov, in: *Proceedings IGARSS'93*, Vol. III, 1091–1093 (1993).
12. *Alt-azimuth solar tracker*, (http://www.brusag.ch/intra.htm)
13. D.K. Davydov, A.P. Plotnikov, and T.K. Sklyadneva, Atmos. Oceanic Opt. **13**, No. 4, 1022–1025 (2000).
14. S.M. Sakerin, in: *Abstracts of Reports at the Third Siberian Conference on Climate-Ecological Monitoring*, Tomsk (1999), pp. 73–74.